INTERACTIONS OF PLANAR WAVES WITH A BAROCLINIC VORTEX IN A ROTATING STRATIFIED FLUID

Frédéric Moulin, Jan-Bert Flór
LEGI, INPG-CNRS-UJF BP 53, 38041 Grenoble Cedex 09 FRANCE

Summary We investigate the interaction of inertia-gravity waves with a baroclinic vortex in a rotating stratified fluid using WKB theory in combination with experimental observations. We show that wave breaking occurs mainly in the periphery of tall vortices, leading to a deposit of momentum, which modifies the vortex velocity profile.

INTRODUCTION

In large-scale geophysical flows, the dominant presence of background rotation and stratification not only prompt the inverse energy-cascade towards large scales, but also support waves e.g. generated during geostrophic adjustment. Here we consider interactions of inertia-gravity waves with a baroclinic vortex in a rotating linearly-stratified fluid, using WKB approach and experimental results. In contrast to most studies on interactions of waves with a unidirectional shear (see e.g. [1]), we consider the interaction of waves with the curved shear of a lenticular vortex.

WKB-APPROACH

To model the wave-vortex interaction with the WKB approach, we consider an isolated lenticular vortex, characterized by a core of constant cyclonic vorticity of radius R embedded in a ring of constant anticyclonic vorticity such that the circulation vanishes at radius L, whereas in the vertical direction a Gaussian vorticity distribution is assumed. Because of stability arguments (see [2]) we take $L = 2R$; the vertical length scale is H, and the amplitude is given by the maximum azimuthal velocity U_{max}. The vortex is in cyclo-geostrophic balance thus setting the density field in accordance with the velocity field. The propagation of inertia-gravity waves can then be described in the framework of the WKB theory by introducing the expressions for density and velocity into the set of ray and refraction equations [3].
The non-dimensional dispersion relationship for the intrinsic frequency ω_0 is a function of the components of the wave vector and the buoyancy frequency field, and reads

$$\omega_o^2 = \frac{N^{*2}(k_r^2 + k_\theta^2) + (f/N_o)^2 k_z^2}{k^2}, \tag{1}$$

where N^* is the buoyancy frequency corrected for the velocity induced density field, and the intrinsic frequency ω_o is a function of the components of the wave vector and the buoyancy frequency field. The non-dimensional form of the Doppler-shift relationship reads

$$\omega_{abs} = \omega_o + \mathrm{Fr}\, k_\theta r \left(\frac{U}{r}\right) \tag{2}$$

with $Fr = U_{max}/(N_0 R)$ the Froude number. In view of this Doppler shift, we distinguish waves propagating in the direction of the azimuthal velocity field of the vortex (briefly $k_\theta > 0$) which experience an increase in intrinsic frequency, and waves propagating against this velocity field (briefly $k_\theta < 0$) which experience a decrease in frequency.
When Fr_w=k Fr $<< 1$, the intrinsic frequency ω_o, and implicitly the orientation of the rays are weakly modified. With increasing Fr_w rays reflect and interact with the vortex. Some rays remain inside the vortex, exhibiting a strong decrease in wave-length associated with the trapping in a critical layer. We use this decrease in wavelength as a criterion to distinguish trapped rays from untrapped waves, and define waves as trapped when the wavelength has decreased to one-tenth of its initial value.
To investigate the effect of the vortex characteristics on the trapping of an ensemble of waves, simulations were carried out for three different aspect ratio H/L, 0.1, 1 and 5 with Fr_w in the range between 0.1 to 1000.0, and ω_{abs} in the range $[f/N_o, 1]$ (and fixed values of the rotation to buoyancy frequency $f/N_o = 0.1$, and $L/R = 2$). To compare the results, we defined a vortex area, σ_{vortex}, seen by incident rays of frequency ω_{abs}. The values $\mathrm{Fr}_w = U_{max}/(N_o\lambda)$, with λ the wavelength, correspond to the same strength in Doppler shift. For a vertically gaussian-shaped vortex of aspect ratio H/R, the non-dimensional form of this expression yields

$$\sigma_{vortex}\left(\omega_{abs}, \frac{H}{R}, \frac{L}{R}\right) = \frac{L}{R}\left(4.0\frac{H}{R}\sqrt{\frac{1-\omega_{abs}^2}{1-(f/N_o)^2}} + \pi\frac{L}{R}\sqrt{\frac{\omega_{abs}^2-(f/N_o)^2}{N^2-(f/N_o)^2}}\right).$$

The trapping area σ is defined as the area of trapped rays divided by the vortex area σ_{vortex} defined above. Generally, rays with low values of Fr_w are not trapped, whereas for higher values of Fr_w trapping area depends on the aspect ratio H/R of the vortex.
For flat vortices, rays propagating with the flow are trapped in the core and periphery by the strong vertical shear, while rays propagating against the flow escape, except very short waves for which the flow curvature in the vortex is negligible.

These rays are trapped near the edge of the vortex, $z = 0$, $r = L$, close to the reflection layer $\omega_o = N$ where the horizontal shear is dominant.

For tall vortices, rays propagating with the flow reflect and escape, whereas waves propagating against the flow are trapped along almost vertical critical layers that are located near the reflection layer $\omega_o = N$. In contrast to flat vortices, all waves with $k_\theta > 0$ escape after reflection in the outer core region (for details see [3]). For increasing Fr_w, the trapping region gets gradually closer to the vortex periphery and increases in energy density. Conservation of wave action flux then leads to an energy amplification, which in real flows leads to breaking or viscous damping by diffusive effects.

EXPERIMENTAL RESULTS

Experimentally, a flat vortex is generated with a thin disk rotating about the vertical axes at mid-depth in the fluid; the vortex is characterized by a core with approximately constant vorticity enclosed by a ring of negative vorticity (for details see [4,6]). A tall vortex is generated by siphoning a given quantity of fluid via a vertical tube over a relatively large depth. After removal of the tube a tall vortex with a velocity profile close to that of a Lamb-Oseen vortex remains. Respectively, quantitative and qualitative information is obtained from PIV measurements and dye or shadow-graph pictures. Comparing the initial and perturbed vortex state for an ensemble of cross-sectional velocity profiles revealed the impact on the velocity profile.

Planar waves propagating against the flow wrap around the vortex while their energy accumulates until their amplitude is high enough to trigger overturning and breaking (see figure 1). For the tall vortex, this wave breaking leads to a deposit of negative momentum in the vortex periphery, and modifies the velocity profile of the vortex from a Lamb-Oseen vortex to an isolated vortex [5,6].

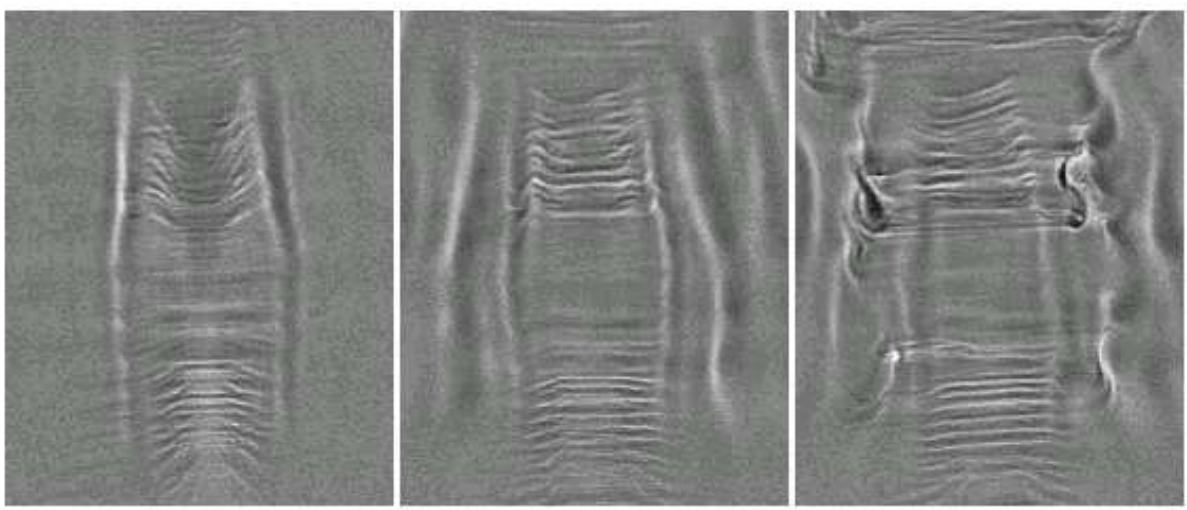

Figure 1. Shadowgraph pictures of inertia gravity waves, emitted by an oscillating cylinder at the right side of the vortex near the bottom, breaking in the shear flow of a tall vortex. The cylinder diameter is $D = 5.0$ cm, while oscillation frequency and amplitude are $0.88 s^{-1}$ and $1.0\ cm$ respectively, and $N_0/f = 1.5$. Times of observation are: 79, 123 and 137 s after forcing.

References

[1] Olbers, 1980, "The propagation of Internal Waves in a geostrophic current". *J. Physical Oceanography* **11**, 1224–1233.
[2] Flierl G.R., 1988, "On the instability of geostrophic vortices". *J. Fluid Mech.* **197**, 349–388.
[3] Moulin, F.Y. & Flór, J.B., 2004, "Vortex wave interaction in a rotating stratified fluid: WKB theory". *J. Fluid Mech.(in preparation).*
[4] Moulin, F.Y. & Flór, J.B., 2004, "On the spin-up by a rotating disk in a rotating stratified fluid". *J. Fluid Mechanics* (accepted).
[5] Moulin, F.Y. & Flór, J.B., 2004, "Experimental study on the wave-breaking and mixing properties of an elongated vortex".*Dyn of Atm. Oceans* (Submitted).
[6] Moulin, F.Y., 2002, PhD-theses. Université Joseph Fourier.